Electrodeposited Prussian Blue on carbon black modified disposable electrodes for direct enzyme-free H_2O_2 sensing in a Parkinson's disease *in vitro* model

Daniel Rojas[a,b], Flavio Della Pelle[a], Michele Del Carlo[a], Michele d'Angelo[c], Reyes Dominguez-Benot[c], Annamaria Cimini[c,d], Alberto Escarpa[b],* Dario Compagnone[a*]

[a] Faculty of Bioscience and Technology for Food, Agriculture and Environment, University of Teramo, 64023, Teramo, Italy

[b] Department of Analytical Chemistry, Physical Chemistry and Chemical Engineering, Faculty of Biology, Environmental Sciences and Chemistry, University of Alcalá, E-28871 Alcalá de Henares, Madrid, Spain

[c]Department of Life, Health and Environmental Sciences, University of L'Aquila, Italy

[d]Sbarro Institute for Cancer Research and Molecular Medicine, Dept of Biology, Temple University, USA.

*Corresponding authors: alberto.escarpa@uah.es, dcompagnone@unite.it

Abstract

In this work, we present the combination of Carbon Black (CB) and electrodeposited Prussian Blue (PB) covered with a Nafion layer on Screen-Printed electrodes (CB/PB-SPE) used for non-enzymatic H_2O_2 sensing in Neuroblastoma cell line SH-SY5Y. These cells were challenged with 6-hidroxidopamine (6-OHDA) for modelling Parkinson's disease. The electrodes surface was investigated using Scanning Electron Microscopy (SEM) and electrochemically characterized, in terms of electroactivity and stability. Electrochemical sensing of H_2O_2 was carried out at very low potentials (-50mV), with a LOD of 0.01 µM and linear range between 0.2 and 1000 µM, allowing interference-free detection of H_2O_2 in the selected cell culture. The H_2O_2 concentration was successfully monitored in an experimental model of Parkinson's disease. These results pave the way to a method for the continuous monitoring of H_2O_2 in culture medium for future studies of the role of H_2O_2 in Parkinson's disease.

Keywords: Prussian Blue, Carbon Black, Hydrogen Peroxide, Screen-Printed electrodes, Parkinson's disease; Cell cultures

1. Introduction

Reactive oxygen species (ROS) are reduced forms of oxygen with important physiological functions and a critical role in redox regulation and oxidative stress development [1,2] The most relevant species are superoxide anion ($O_2^{\cdot-}$), hydroxyl radical ($OH^{\cdot}$) and hydrogen peroxide (H_2O_2) which are products of the normal metabolic consumption of oxygen. The main sources of ROS in aerobic cells can be related to membrane-bound NADPH oxidase and to incomplete oxygen reduction in mitochondria [3]. However, there are other pathways of generation of ROS such as ionizing radiation, Fenton and Haber-Weiss reaction of transition metal ions, drugs as antibiotics and chemotherapeutics [4]. Oxidative Stress (OS) is described as the imbalance between the production of oxidants (mainly ROS) and antioxidants defences. Some situations may favour this imbalance, for instance, disfunction of antioxidant enzymes, exposure to some chemicals able to produce ROS, decrease in the levels or production of low molecular mass antioxidants and antioxidant enzymes [5]. This status can cause disruption in redox signalling and/or molecular damage. OS occurs when production of ROS/RNS is in excess with respect to the antioxidant protecting capacity; this causes irreversible damages to proteins, DNA and lipids. These biochemical alterations are implicated in several pathological processes such as cancer, Parkinson's and Alzheimer's disease, ischemia [6], atherosclerosis [7] and, in general, aging [8]. However, little amounts of ROS are necessary for the correct functioning of immunodefenses and redox signalling; the latter is denominated as a "oxidative eustress" [2]. Therefore, there is a need for analytical methods, possibly allowing continuous monitoring of ROS markers in cell cultures to evaluate the OS level in cells with respect to different treatments. Among the cellular produced ROS, H_2O_2 is the most representative in terms of amounts and half-life, and, therefore, the most studied.

Parkinson's disease (PD) involves an irreversible degeneration of the nigrostriatal dopaminergic pathway, resulting in an evident impairment of motor control. Although the etiology of PD remains unknown, recent studies have suggested that oxidative stress is an important mediator in this pathogenesis [9]. It is hypothesized that nigral dopaminergic neurons are exposed to high ROS levels, due to the metabolism of dopamine itself (both enzymatic and nonenzymatic) leading to the generation of ROS, including superoxide anion, hydrogen peroxide (H_2O_2) and hydroxyl radicals. In fact, there are several indirect observations, such as the increased levels of the oxidation products of lipids, proteins, and nuclear acids in nigral cells, that are indicative of the role of oxidative stress in PD [10]. Hydroxydopamine (6-OHDA) is a selective catecholaminergic neurotoxin that has been widely used to produce PD models in vitro and in vivo; it induces a toxicity status that mimics the neuropathological and biochemical characteristics of PD [11]. It has been reported that 6-OHDA is oxidized rapidly by molecular oxygen to form the superoxide anion, hydrogen peroxide, and 2-hydroxy-5-(2-aminoethyl)-1,4-benzoquinone (p-quinone) as follows [12]:

$$\text{6-OHDA} + O_2 \rightarrow \text{p-quinone} + H_2O_2 \quad (1)$$

It is well known that the ROS generated from 6-OHDA initiate cellular oxidative stress. On the other hand, it has been reported that p-quinone mediates 6-OHDA-induced cell death [13]. However, the exact mechanisms of ROS production and neurotoxicity induction, particularly in relation to caspase activation, are less clearly defined. Based on the above description, in this work, we considered important the evaluation the H_2O_2 production after the exposure at 6-OHDA on the PD in vitro model; in this way, we can better understand the neurotoxic effect of this ROS at different timing.

Different analytical strategies have been proposed for H_2O_2 detection such as chemiluminescence,[14] fluorescence,[15,16] and electrochemical techniques [17]. Among these, electrochemical sensors are very appealing for their simplicity, speed, sensitivity, miniaturization and cost-effectiveness [18]. In the past two decades biosensors have dominated the sensors scenario even in the ROS detection field [17,19], while in the last decade nanomaterials have become alternative/ complementary sensor useful tools [20–24]. Indeed, nanostructured sensors allow to improve the sensitivity and selectivity providing larger surface area and faster electron transfers in comparison with their bulk counterparts [21,25,26]. Hence, the combination of nanomaterials and electrochemical sensors is very attractive. Direct sensing of H_2O_2 in classical metal electrodes such as platinum or gold is possible, however, it suffers from poor selectivity due to the high overpotentials needed. The selection of a proper nanomaterial and catalyst can overcome this drawback. Prussian Blue (PB), also known as “artificial peroxidase” [27] is one of the most known and widely used electrocatalyst for H_2O_2 reduction. PB allows low potential and interference-free detection of H_2O_2 in oxygenated media; nonetheless, has some disadvantages such as poor stability at physiological pH and high crystallization rate which hinder the potential use in nanocomposites and

application in biological media [28]. To overcome these shortcomings, electrode modification with soft or hard templates, polymers, carbonaceous materials or different metals have been used in different combinations to build specific analytical platforms for each application [19]. Carbon Black (CB) is a carbon nanomaterial widely used as reinforcing material and as filler in the preparation of rubber and plastic compounds and composites, made by petroleum products combustion so it is a very cheap carbonaceous nanomaterial (about 1€/Kg). It is characterized by a primary structure constituted of spherical particles with diameter between 30 and 100 nm and a secondary structure formed by aggregates having dimensions in the range of 100–600 nm [29]. CB dispersions after sonication, in appropriate solvents, appears as carbon nanoparticles. Recent data reported that modified electrodes based on CB present fast charge transfer and high electroactive area, comparable to carbon nanotubes and graphene [30]. These characteristics in conjunction with the extremely low cost make CB a promising candidate for the design of electrochemical sensors and biosensors. In this respect CB can be clearly considered a good alternative to carbon nanotubes and graphene. For these reasons, in the last years several works have been reported on the CB dispersion for electrode modification, showing remarkable electrocatalytic properties towards several species of analytical interest [20,30–33], allowing the realization of new electrochemical devices devices [34–36]. In this work 'nano CB' has been successfully used as electrode modifier for the controlled electrodeposition of PB and further applied for the monitoring of H_2O_2 in Parkinson's disease cellular model cultures.

2. Experimental

2.1. Materials

Experiments were carried out with MilliQ water from a Millipore MilliQ ((Millipore, Bedford, MA, USA), system. All inorganic salts, 6-OHDA, organic solvents and hydrogen peroxide (30% solution) were obtained at the highest purity from Sigma-Aldrich. SHSY5Y cells were obtained from Sigma (Sigma–Aldrich). Catalase from bovine liver powder, suitable for cell culture, 2,000-5,000 units/mg protein was purchased from Sigma-Aldrich (C1345). H2O2 concentration was periodically standardized by titration with KMnO4. Screen-Printed electrodes (SPE) were purchased from Dropsens S.L. (ref. DS110). DMEM, L-Glutamine, penicillin/streptomycin, trypsin and flask were purchased from Corning (Corning Life Sciences, Corning, NY).

2.2. Instrumentation

All electrochemical measurements were carried out in Autolab PGSTAT 12 potentiostat from Metrohm (Utrecht, The Netherlands) connected to a personal computer. The software used was the Nova 2.1 (EcoChemie B.V.). The flow injection (FIA) system consisted on a Minipuls 3 (Gilson Inc., Middleton, WI, USA) peristaltic pump, flow-through cell (ref. FLWCL) (Dropsens, Spain). Sample volume was 50 µL, the working electrode potential chosen was -50 mV (vs internal reference). The running buffer solution in FIA experiments was 0.05 M phosphate buffer pH 7.4 containing 0.1 M KCl. High resolution scanning

electron microscopy (HR-SEM) was carried out on the materials using a Zeiss Auriga HR- SEM. The scanning electron microscopy, Zeiss Auriga, High resolution FESEM was used to study the morphology of the prepared materials.

2.3. Preparation of PB and CB-PB electrodes

A CBNPs dispersion of 1 mg/mL in water and dimethylformamide (DMF) (1:1 ratio). The dispersions were obtained using a bath sonicator for 30 min. Further, commercially screen-printed electrodes (DS110) were modified via drop-casting using different volumes (from 3.5 µL to 35 µL). The amount of CB was optimized checking the reversibility of $[Fe(CN)_6]^{3-/4-}$ couple using cyclic voltammetry and charge transfer resistance (Rct) in electrochemical impedance spectroscopy (EIS). The selected optimum value was 10 µL drop-casted by 1 µL each time (**Fig. S.1**). Prussian Blue electrodeposition was carried out cycling the potentials between +400 and +800 mV (vs int. ref) for different number of cycles in a solution containing solution containing 0.1 M KCl, 0.1 M HCl and 5mM concentration of Fe^{3+} and $[Fe(CN)_6]^{3-}$. The potential of the internal reference electrode against an $Ag|AgCl|KCl_{sat}$ reference electrode was measured as -120 mV. Electrodes were further modified with 2 µL of a Nafion ethanolic solution (0,5% v/v). Nafion is an ionic conductor that increase stability of PB modified electrodes, allowing the counterions transport to maintain the electroneutrality of PB [37,38].

.

2.4. Cell culture.

The Neuroblastoma cell line SH-SY5Y were maintained at 37°C in a 5% CO2 humidified atmosphere in DMEM medium supplemented with 10% heat-inactivated fetal bovine serum, 2 mM L-Glutamine, 0.2 mg/ml penicillin/streptomycin. The culture medium was changed every 2 days until cells reached approximately 70–80% confluency. Cells were harvested using 0.25% trypsin-0.53 mM EDTA solution and were seeded at approximately 4×104 cells/cm^2 in 75 cm^2-flasks, then treated with 6 OHDA (50µM) for different times.

2.5. Cell viability

Cells were seeded (5.000 cells/well) in a 96 wells plate, the day after the cells were treated with 6 OHDA (50 µM) for 24 h while the control cells received only DMEM containing 10% of FBS, every treatment was performed in quintuplicate. The cells were incubated for different time and at expiration of incubation period cell viability was determined using Cell Titer One Solution Cell Proliferation Assay reading the absorbance at 492 nm, in a spectrophotometric microplate reader Infinite F200 (Tecan, Männedorf, Swiss). The results were expressed as absorbance recorded at 492 nm.

3. Results and Discussion

3.1. Preparation and characterization of CB-PBNPs electrodes

PB or ferric ferrocyanide is one of the oldest know coordination compound with ferric ions coordinated to nitrogen and ferrous coordinated to carbon in a face

centered cubic lattice. Usually, is electrochemically deposited using a mixture of Fe^{3+} and $[Fe(CN)_6]^{3-}$ where the ferric ions are reduced to form Prussian Blue. Particular attention has to be paid to the selection of the potential used for the electrodeposition; in fact, the concurrent reduction of both precursors leads to an irregular structure of the Prussian Blue layer onto the electrode surface [27]. As shown in the cyclic voltammogram of **Fig. 1A**, the reduction peaks of Fe^{3+} and $[Fe(CN)_6]^{3-}$ are not resolved using bare SPE. Interestingly, in the case of CB-SPE the peak potential of Fe^{3+} is anodical shifted 280 mV, and peak current is increased by a 1.5 factor confirming an electrocatalytic behaviour of CB toward Fe^{3+} reduction. On the other hand, for the reduction of $[Fe(CN)_6]^{3-}$, only a slight increase of peak intensity was observed, keeping the peak potential at the same value of unmodified SPE. Thus, the electrodeposition of PB was carried out using cycling voltammetry; the potential window and the sweep rate was selected according to the method developed by Karyakin et al [27,39]. Considering the reported electrochemical behaviour of the electrodes surface SPE were cycled from +400 mV to +800 mV (vs. Ag), allowing the selective reduction of Fe^{3+} keeping the $[Fe(CN)_6]^{3-}$ in its oxidized form. **Fig. 1B** reports cyclic voltammograms in a solution containing 0.1M HCl and 0.1M KCl. An increase in the peak current and area was observed with number of electrodeposition cycles indicating a higher quantity of PB on the electrode surface. It is clearly noticeable the higher electrodeposited quantity at CB-modified electrodes compared to the bare SPE. The electrocalitic activity of SPE-CB/PB is reported in Fig. S.2A; using amperometric detection, the combination of SPE-CB and PB results in a a higher signal for H_2O_2 reduction compared to SPE-PB and SPE-CB as shown in Fig. S.2B. In carbon-based electrodes, the only available detection principle is H_2O_2 oxidation at high anodic potential, where easily oxidizable compounds usually presents in biological media causes appearance of parasitic signal due their oxidation. In contrast, PB-based electrodes allow H_2O_2 detection by reduction near 0V (vs Ag|AgCl), where other compounds are rarely electroactive.

SEM micrographs confirmed the growth of PB onto the electrode surface. As reported in **Fig.2**, increasing the number of electrodeposition cycles, the size of the PB nanoparticles increases. In addition, the amount of atomic iron, obtained from EDS spectra was found to be from 0 to 3.55% CB-SPE up to 20 cycles.

Table 1 list the surface coverage (Γ) of PB as well as $S \cdot t_{95\%}$ as sensor stability and sensitivity parameter. High stability and electrocatalytic activity is highly desirable to obtain. However, it is not trivial to find a compromise between the two characteristics. For this purpose an accelerated degradation can be carried out [40]. Sensor's stability is evaluated by the time the measured current reaches the 95% of its initial value ($t_{95\%}$) under continuous flow of 500 µM H_2O_2 in Phosphate Buffer pH=7.4 using a wall-jet cell. Sensitivity (S) is estimated by the initial intensity divided by the concentration of H_2O_2.

Table 1: Optimization parameter for CB-PB electrodes

Electrode	Γ (nmol·cm^{-2})	$S \cdot t_{95\%}$ (A·min·M^{-1}·cm^{-2})
CB-PB- 5 cycles	0.85	1.83

CB-PB- 10 cycles	3.90	4.69
CB-PB- 20 cycles	6.40	4.59

As shown in **Table 1**, as we increased the surface coverage (Γ) of PB the parameter $S \cdot t_{95\%}$ raises from 5 to 10 cycles and slightly decreases from 10 to 20 cycles. Therefore, considering the values of $S \cdot t_{95\%}$ the compromise among sensitivity and stability of the sensor is found with 10 cycles of electrosynthesis.

3.2. Analytical performance

The selected electrode was used for the electrochemical detection of H_2O_2 in a Flow Injection Analysis (FIA) system. FIA was chosen as a first approach for quantifying H_2O_2 in cell cultures, taking advantage of its high throughput, simplicity and possibility to automation. In order to find the optimal conditions for measuring, an optimization of the flow rate and potential employed in the analysis was carried out. **Fig. 3A** shows the effect of the flow rate on the peak intensity of a solution containing 10 µM of H_2O_2. An increase in the flow rate increases the peak intensity until it reaches a constant value at a flow rate of 0.6 ml min^{-1} and above. Hydrodynamic voltammogram of CB-PB electrodes in phosphate buffer and phosphate buffer containing 100 µM of H_2O_2 in aerated solution were also carried out. As shown in **Fig.3B** the current in presence of H_2O_2 reaches the limiting current at -50 mV. In addition, the selectivity of the electrodes in presence of oxygen, a common interferent using platinum or gold electrodes, is demonstrated as we have negligible current from the aerated buffer at the region of the limiting current for H_2O_2 reduction.

The electrochemical performance of the electrodes was then tested in FIA analysis of hydrogen peroxide in hydrogen phosphate buffer pH = 7.4. Physiological pH is not the ideal pH for PB-based sensors; however, we obtained satisfactory data. **Fig. 4A** reports the amperometric response of the developed sensor for the injection of different H_2O_2 concentrations ranging from 200 nM to 1 mM. Linearity was found over 4 orders of magnitude, as shown in **Fig. 4B**. The equation of calibration curve was: i_p=0,039±0,007(µM)+ 0.66±0.01($A \cdot M^{-1} \cdot cm^{-2}$)[$H_2O_2$] with R^2= 0.999. The limit of detection, calculated as 3σ/S, where σ is the standard deviation of 10 blank samples and S the sensitivity, was 10 nM. In addition, good intra-electrode repeatability and inter-electrode reproducibility were obtained RSD≤6% (n=3) and RSD≤10%(n=5), respectively.

To the best of our knowledge, the combination of CB/PB and SPE to construct a H_2O_2 sensor has previously been used only by Cinti et al. [41]. In this work, different combinations of CB/PB composites were synthetized producing different PB nanoparticles sizes; LODs were between 0.3 and 1.0 µM and sensitivities between 0.15-0.56 $A \cdot M^{-1} \cdot cm^{-2}$ using amperometry batch analysis. Our proposed electrode has a lower LOD and improved sensitivity (0.66 $A \cdot M^{-1} \cdot cm^{-2}$) and takes advantage of the measurement FIA system which allows a higher throughput (70 samples$\cdot h^{-1}$) and better repeatability. In addition, the SPE-CB/PB retained the analytical performance, in terms of sensitivity, (87% after 3 months at RT) demonstrating a good long-term stability.

3.3. Application to H_2O_2 sensing in SHSY5Y differentiated in neurons cell cultures

Cellular culture medium is a quite complex and challenging matrix since contains different organic compounds and proteins necessary for the cells. Matrix effect must be carefully assessed in order to produce reliable quantitative data. The sample matrix has been spiked with known amounts of H_2O_2 in the 5 - 50 µmol L^{-1} concentration range. The recovery was in the whole range ≥96% with RSD≤4% (n=3). These data show that the procedure is suitable for H_2O_2 detection in cellular culture. Selectivity of the measurements was also evaluated vs. possible interferents found in the culture broth. To this aim the influence of Penicilin, Streptavidin, L-Glutamine and Fetal Bovine Serum have been studied. As reported in **Fig.5A** no significant interference was observed. In addition, we have further tested the selectivity of our electrode against the H_2O_2 reduction in the complex matrix. As it is observed in **Fig.5B**, the signal due to the addition of 100 µM H_2O_2 in the cell culture media was completely suppressed by the addition of 0.2 mg of Catalase (100 µL 2 mg/ml). It should be also noticed that the sensor was able to measure in the DMEM cell culture for 1h maintaining the 80% of the initial signal in batch amperometry configuration, exhibiting an excellent stability in such complex media; this remarkable feature allows the use of such low-cost sensors as the modified SPE for a large number of measurements/experiments with cells.

Finally, the proposed strategy has been successfully applied to monitor in Parkinson's cellular culture H_2O_2 production (for 24 hours). Cells were stimulated by 6-OHDA, a selective catecholaminergic neurotoxin, which has been frequently used to create PD models. The toxic effect of 6-OHDA is mediated by its uptake into catecholaminergic nerve endings via the high-affinity catecholamine transporter system. Several works report that 6-OHDA triggers cell death through three main mechanisms: a) ROS generation through autoxidation, b) H_2O_2 generation following deamination by monoamine oxidase (MAO), c) direct inhibition of mitochondrial complexes I and IV [42]. However, many recent studies have reported that 6-OHDA does not induce toxicity either by direct mitochondrial inhibition or by enzymatic deamination by MAO, but through an extracellular mechanism [11,43]. The sample analysis was carried out in a flow injection system with the optimized Prussian Blue/ Carbon Black modified Screen Printed Electrode as detection system and using the following procedure: 1) injection of a known standard sample (triplicate) 2) Injection of sample (triplicate). The standard injections allow us to normalize the signal minimising, any matrix effect or change of the electrodes in the FIA setup. H_2O_2 amount found in the cell culture increases as a function of the incubation time, reaching a plateau-like region at 20h (**Fig.6)**. The concentration ranges were from 15.2 ± 0.8 µM at 15 min to 51.9 ± 0.3 µM at 24h, which are in accordance with values found in literature for the 6-OHDA model [44]. In this preliminary experiment, we demonstrate the relationship between an overproduction of H_2O_2 after 6-OHDA treatment with the high mortality evaluated with MTS viability assay (**Fig. 6**). In fact, we observed an increase of cell mortality linked to H_2O_2 concentration.

The analytical performance of other nanomaterials based electrochemical sensors used for measuring hydrogen peroxide in cell culture is reported in Table 2. The developed electrode showed better or comparable analytical performance compared with works found in the literature in terms of LOD and linear range, even compared with noble metals-based sensors. It is important to note that the developed electrode consist in a SPE which has inherent advantages compared to classic solid electrode such as disposability, ease of use and low sample consumption. When compared with other SPE (SPE-Cu-NWs), we found lower LOD, wider linear range and the detection potential closer to 0 mV (vs Ag/AgCL). In addition, to the best of our knowledge, this is the first time that H_2O_2 is measured and quantified in the 6-OHDA model for Parkinson's disease using electrochemical sensors.

Table 2: Comparison of analytical performance of hydrogen peroxide sensors applied to the determination of hydrogen peroxide released by cells

Electrode	Detection potential (mV)	LOD (M)	Linear range (M)	Application	Ref
Au-PB-PDA	+100 vs Ag/AgCl	$1.0x10^{-7}$	$1.0x10^{-6}$-$8.0x10^{-4}$	Hep G2 cells	[45]
SPE-Cu-NWs	-200 vs Ag	$4.0x10^{-7}$	$5.0x10^{-7}$-$8.0x10^{-4}$	Cisplatin-treated human renal HK-2 cells	[24]
g-CNTs/PB MCs	-50 vs Ag|AgCl, sat KCl	$1.3x10^{-8}$	$2.5x10^{-8}$-$1.6x10^{-3}$	RAW 264.7 cells	[46]
Pd/Au NWs	-50 vs Ag|AgCl, 3M KCl	$3.0x10^{-7}$	$1.0x10^{-6}$-$1.0x10^{-3}$	HL-1 cells	[47]
PtPb/Graphene	-200 vs Ag|AgCl	$2.0x10^{-9}$	$2.0x10^{-9}$-$2.5x10^{-3}$	Raw 264.7 cells	[48]
CuO@MnAl LDHs	-850 vs SCE	$1.3x10^{-7}$	$6.0x10^{-6}$-$22x10^{-3}$	Epithelial normal cells HBL100, breast cancer cells MCF-7 and glioma brain cancer cells U87	[49]
PdPt NCs@SGN/GCE	-0.1 vs SCE	$3.0x10^{-7}$	$3.0x10^{-6}$-$3.0x10^{-4}$	Hela cells	[50]
Ag NSs/GCE	-500 vs Ag|AgCl, sat KCl	$1.7x10^{-7}$	$5.0x10^{-6}$-$6.0x10^{-3}$	HeLa cells and SH-SY5Y cells	[51]
SPE-CB-PB-Nafion	-50 mV vs Ag	$1.0x10^{-8}$	$2.0x10^{-7}$-$1.0x10^{-3}$	Neuroblastoma SH-SY5Y cell line	This work

4. Conclusions

An enzyme-free electrochemical sensing platform was successfully proposed for the quantification of H_2O_2 released by SHSY5Y cells. These cells challenged to 6-OHDA represent a model to study the Parkinson's disease, which is widely known to be affected by oxidative stress. To the best of our knowledge, this is the first time that an electrochemical PB/CB sensor is applied to sensing H_2O_2 directly in cell cultures. The described sensor showed detection limit in the nanomolar range and showed excellent selectivity in a complex environment such as the culture medium used, allowing the selective determination of very low amounts of H_2O_2 without interferences. In addition, in this work H_2O_2 was quantified instead of following its almost instantaneous release from cells challenged to a stressor in contrast to [45] and [46]. These results could pave

the way for a better understanding the neurotoxic effect of ROS using an in vitro model of Parkinson's disease.

5. Acknowledgements

This work is supported by funding from the European Union's Horizon 2020 research and innovation programme under the Marie Skłodowska-Curie grant agreement Nº 713714 and co-funding of University of Teramo and Abruzzo region.

6. Bibliography

[1] H. Sies, C. Berndt, D.P. Jones, Oxidative Stress, Annu. Rev. Biochem. 86 (2017) 715–748. doi:10.1146/annurev-biochem-061516-045037.

[2] H. Sies, Hydrogen peroxide as a central redox signaling molecule in physiological oxidative stress: Oxidative eustress, Redox Biol. 11 (2017). doi:10.1016/j.redox.2016.12.035.

[3] C.R. Reczek, N.S. Chandel, The Two Faces of Reactive Oxygen Species in Cancer, Annu. Rev. Cancer Biol. 1 (2017) 79–98. doi:10.1146/annurev-cancerbio-041916-065808.

[4] A. Umeno, V. Biju, Y. Yoshida, In vivo ROS production and use of oxidative stress- derived biomarkers to detect the onset of diseases such as Alzheimer ' s disease , Parkinson ' s disease , and diabetes, Free Radic. Res. 5762 (2017). doi:10.1080/10715762.2017.1315114.

[5] V.I. Lushchak, Free radicals, reactive oxygen species, oxidative stress and its classification, Chem. Biol. Interact. 224 (2014) 164–175. doi:10.1016/j.cbi.2014.10.016.

[6] C. Espinosa-Diez, V. Miguel, D. Mennerich, T. Kietzmann, P. Sánchez-Pérez, S. Cadenas, S. Lamas, Antioxidant responses and cellular adjustments to oxidative stress, Redox Biol. 6 (2015) 183–197. doi:10.1016/J.REDOX.2015.07.008.

[7] A.J. Kattoor, N.V.K. Pothineni, D. Palagiri, J.L. Mehta, Oxidative Stress in Atherosclerosis, Curr. Atheroscler. Rep. 19 (2017). doi:10.1007/s11883-017-0678-6.

[8] S.I. Liochev, Reactive oxygen species and the free radical theory of aging, Free Radic. Biol. Med. 60 (2013) 1–4. doi:10.1016/j.freeradbiomed.2013.02.011.

[9] H. Sies, Oxidative stress: From basic research to clinical application, Am. J. Med. 91 (1991) S31–S38. doi:10.1016/0002-9343(91)90281-2.

[10] A. Miyama, Y. Saito, K. Yamanaka, K. Hayashi, T. Hamakubo, N. Noguchi, Oxidation of DJ-1 Induced by 6-Hydroxydopamine Decreasing Intracellular Glutathione, PLoS One. 6 (2011) e27883. doi:10.1371/journal.pone.0027883.

[11] Y. Saito, K. Nishio, Y. Ogawa, T. Kinumi, Y. Yoshida, Molecular mechanisms of 6-hydroxydopamine-induced cytotoxicity in PC12 cells : Involvement of hydrogen peroxide-dependent and -independent action, 42 (2007) 675–685. doi:10.1016/j.freeradbiomed.2006.12.004.

[12] G. Cohen, R.E. Heikkila, Generation of Hydrogen-Peroxide, Superoxide Radical, and Hydroxyl Radical by 6-Hydroxydopamine, Dialuric Acid, and Related Cytotoxic Agents, J. Biol. Chem. 249 (1974) 2447–2452.

[13] Y. Izumi, H. Sawada, N. Sakka, N. Yamamoto, T. Kume, H. Katsuki, S. Shimohama, A. Akaike, p-quinone mediates 6-hydroxydopamine-induced dopaminergic neuronal death and ferrous iron accelerates the conversion

ofp-quinone into melanin extracellularly, J. Neurosci. Res. 79 (2005) 849–860. doi:10.1002/jnr.20382.

[14] W. Vessey, A. Perez-Miranda, R. Macfarquhar, A. Agarwal, S. Homa, Reactive oxygen species in human semen: Validation and qualification of a chemiluminescence assay, Fertil. Steril. 102 (2014) 1576–1583. doi:10.1016/j.fertnstert.2014.09.009.

[15] A.-C. Ribou, Synthetic Sensors for Reactive Oxygen Species Detection and Quantification: A Critical Review of Current Methods, Antioxid. Redox Signal. 25 (2016) 520–533. doi:10.1089/ars.2016.6741.

[16] N. Burmistrova, O. Kolontaeva, A. Duerkop, New Nanomaterials and Luminescent Optical Sensors for Detection of Hydrogen Peroxide, Chemosensors. 3 (2015) 253–273. doi:10.3390/chemosensors3040253.

[17] H. Liu, L. Weng, C. Yang, A review on nanomaterial-based electrochemical sensors for H2O2, H2S and NO inside cells or released by cells, Microchim. Acta. 184 (2017) 1267–1283. doi:10.1007/s00604-017-2179-2.

[18] Z. Li, Y. Yu, Z. Li, T. Wu, J. Yin, The art of signal transforming: electrodes and their smart applications in electrochemical sensing, Anal. Methods. 7 (2015) 9732–9743. doi:10.1039/C5AY02373D.

[19] C. Calas-Blanchard, G. Catanante, T. Noguer, Electrochemical Sensor and Biosensor Strategies for ROS/RNS Detection in Biological Systems, Electroanalysis. 26 (2014) 1277–1286. doi:10.1002/elan.201400083.

[20] F. Della Pelle, D. Compagnone, Nanomaterial-Based Sensing and Biosensing of Phenolic Compounds and Related Antioxidant Capacity in Food, Sensors. 18 (2018) 462. doi:10.3390/s18020462.

[21] F.S. Ligler, H.S. White, Nanomaterials in analytical chemistry, Anal. Chem. 85 (2013) 11161–11162. doi:10.1021/ac403331m.

[22] J. Sun, H. Sun, Z. Liang, Nanomaterials in Electrochemiluminescence Sensors, ChemElectroChem. 4 (2017) 1651–1662. doi:10.1002/celc.201600920.

[23] G. Maduraiveeran, W. Jin, Nanomaterials based electrochemical sensor and biosensor platforms for environmental applications, Trends Environ. Anal. Chem. 13 (2017) 10–23. doi:10.1016/J.TEAC.2017.02.001.

[24] L. García-Carmona, M. Moreno-Guzmán, A. Martín, S. Benito Martínez, A.B. Fernández-Martínez, M.C. González, J. Lucio-Cazaña, A. Escarpa, Aligned copper nanowires as a cut-and-paste exclusive electrochemical transducer for free-enzyme highly selective quantification of intracellular hydrogen peroxide in cisplatin-treated cells, Biosens. Bioelectron. 96 (2017) 146–151. doi:10.1016/j.bios.2017.04.048.

[25] M. Pumera, A. Escarpa, Nanomaterials as electrochemical detectors in microfluidics and CE: Fundamentals, designs, and applications, Electrophoresis. 30 (2009) 3315–3323. doi:10.1002/elps.200900008.

[26] A. Escarpa, Lights and shadows on Food Microfluidics, Lab Chip. 14

(2014) 3213–3224. doi:10.1039/C4LC00172A.

[27] A.A. Karyakin, Advances of Prussian blue and its analogues in (bio)sensors, Curr. Opin. Electrochem. (2017). doi:10.1016/j.coelec.2017.07.006.

[28] Z. Chu, Y. Liu, W. Jin, Recent progress in Prussian blue films: Methods used to control regular nanostructures for electrochemical biosensing applications, Biosens. Bioelectron. 96 (2017) 17–25. doi:10.1016/j.bios.2017.04.036.

[29] F. Arduini, A. Amine, C. Majorani, F. Di Giorgio, D. De Felicis, F. Cataldo, D. Moscone, G. Palleschi, High performance electrochemical sensor based on modified screen-printed electrodes with cost-effective dispersion of nanostructured carbon black, Electrochem. Commun. 12 (2010) 346–350. doi:10.1016/j.elecom.2009.12.028.

[30] T.A. Silva, F.C. Moraes, B.C. Janegitz, O. Fatibello-filho, R.W. Lu, Electrochemical Biosensors Based on Nanostructured Carbon Black : A Review, 2017 (2017). doi:https://doi.org/10.1155/2017/4571614.

[31] F. Della Pelle, M. Del Carlo, M. Sergi, D. Compagnone, A. Escarpa, Press-transferred carbon black nanoparticles on board of microfluidic chips for rapid and sensitive amperometric determination of phenyl carbamate pesticides in environmental samples, Microchim. Acta. 183 (2016) 3143–3149. doi:10.1007/s00604-016-1964-7.

[32] F. Arduini, S. Cinti, V. Scognamiglio, D. Moscone, Nanomaterials in electrochemical biosensors for pesticide detection: advances and challenges in food analysis, Microchim. Acta. 183 (2016) 2063–2083. doi:10.1007/s00604-016-1858-8.

[33] F. Della Pelle, C. Angelini, M. Sergi, M. Del Carlo, A. Pepe, D. Compagnone, Nano carbon black-based screen printed sensor for carbofuran, isoprocarb, carbaryl and fenobucarb detection: application to grain samples, Talanta. 186 (2018) 389–396. doi:10.1016/j.talanta.2018.04.082.

[34] S. Cinti, M. Basso, D. Moscone, F. Arduini, A paper-based nanomodified electrochemical biosensor for ethanol detection in beers, Anal. Chim. Acta. 960 (2017) 123–130. doi:10.1016/j.aca.2017.01.010.

[35] F. Della Pelle, R. Di Battista, L. Vázquez, F.J. Palomares, M. Del Carlo, M. Sergi, D. Compagnone, A. Escarpa, Press-transferred carbon black nanoparticles for class-selective antioxidant electrochemical detection, Appl. Mater. Today. 9 (2017) 29–36. doi:10.1016/J.APMT.2017.04.012.

[36] F. Della Pelle, L. Vázquez, M. Del Carlo, M. Sergi, D. Compagnone, A. Escarpa, Press-Printed Conductive Carbon Black Nanoparticle Films for Molecular Detection at the Microscale, Chem. - A Eur. J. 22 (2016) 12761–12766. doi:10.1002/chem.201601743.

[37] F. Ricci, G. Palleschi, Sensor and biosensor preparation, optimisation and applications of Prussian Blue modified electrodes, Biosens. Bioelectron. 21 (2005) 389–407. doi:10.1016/j.bios.2004.12.001.

[38] J.J. García-Jareño, J. Navarro-Laboulais, F. Vicente, Electrochemical study of Nafion membranes/Prussian blue films on ITO electrodes, Electrochim. Acta. 41 (1996) 2675–2682. doi:10.1016/0013-4686(96)00121-1.

[39] A.A. Karyakin, E.A. Puganova, I.A. Budashov, I.N. Kurochkin, E.E. Karyakina, V.A. Levchenko, V.N. Matveyenko, S.D. Varfolomeyev, Prussian Blue Based Nanoelectrode Arrays for H_2O_2 Detection, Anal. Chem. 76 (2004) 474–478. doi:10.1021/ac034859l.

[40] E. V. Karpova, E.E. Karyakina, A.A. Karyakin, Iron–nickel hexacyanoferrate bilayer as an advanced electrocatalyst for H 2 O 2 reduction, RSC Adv. 6 (2016) 103328–103331. doi:10.1039/C6RA24128J.

[41] S. Cinti, F. Arduini, G. Vellucci, I. Cacciotti, F. Nanni, D. Moscone, Carbon black assisted tailoring of Prussian Blue nanoparticles to tune sensitivity and detection limit towards H2O2 by using screen-printed electrode, Electrochem. Commun. 47 (2014) 63–66. doi:10.1016/J.ELECOM.2014.07.018.

[42] D. Blum, S. Torch, N. Lambeng, M.-F. Nissou, A.-L. Benabid, R. Sadoul, J.-M. Verna, Molecular pathways involved in the neurotoxicity of 6-OHDA, dopamine and MPTP: contribution to the apoptotic theory in Parkinson's disease, Prog. Neurobiol. 65 (2001) 135–172. doi:10.1016/S0301-0082(01)00003-X.

[43] K. Hanrott, L. Gudmunsen, M.J. O'Neill, S. Wonnacott, 6-Hydroxydopamine-induced Apoptosis Is Mediated via Extracellular Auto-oxidation and Caspase 3-dependent Activation of Protein Kinase Cδ, J. Biol. Chem. 281 (2006) 5373–5382. doi:10.1074/jbc.M511560200.

[44] Y. Saito, K. Nishio, Y. Ogawa, T. Kinumi, Y. Yoshida, Y. Masuo, E. Niki, Molecular mechanisms of 6-hydroxydopamine-induced cytotoxicity in PC12 cells: Involvement of hydrogen peroxide-dependent and -independent action, Free Radic. Biol. Med. 42 (2007) 675–685. doi:10.1016/J.FREERADBIOMED.2006.12.004.

[45] R. Li, X. Liu, W. Qiu, M. Zhang, In Vivo Monitoring of H2O2 with Polydopamine and Prussian Blue-coated Microelectrode, Anal. Chem. 88 (2016) 7769–7776. doi:10.1021/acs.analchem.6b01765.

[46] T.S.T. Balamurugan, V. Mani, C.-C. Hsieh, S.-T. Huang, T.-K. Peng, H.-Y. Lin, Real-time tracking and quantification of endogenous hydrogen peroxide production in living cells using graphenated carbon nanotubes supported Prussian blue cubes, Sensors Actuators B Chem. 257 (2018) 220–227. doi:10.1016/J.SNB.2017.10.151.

[47] K.G. Nikolaev, V. Maybeck, E. Neumann, S.S. Ermakov, Y.E. Ermolenko, A. Offenhäusser, Y.G. Mourzina, Bimetallic nanowire sensors for extracellular electrochemical hydrogen peroxide detection in HL-1 cell culture, J. Solid State Electrochem. 22 (2018) 1023–1035. doi:10.1007/s10008-017-3829-3.

[48] Y. Sun, M. Luo, X. Meng, J. Xiang, L. Wang, Q. Ren, S. Guo, Graphene/Intermetallic PtPb Nanoplates Composites for Boosting Electrochemical Detection of H_2O_2 Released from Cells, Anal. Chem. 89 (2017) 3761–3767. doi:10.1021/acs.analchem.7b00248.

[49] M. Asif, W. Haitao, D. Shuang, A. Aziz, G. Zhang, F. Xiao, H. Liu, Metal oxide intercalated layered double hydroxide nanosphere: With enhanced electrocatalyic activity towards H2O2 for biological applications, Sensors Actuators B Chem. 239 (2017) 243–252. doi:10.1016/J.SNB.2016.08.010.

[50] Y. Fu, D. Huang, C. Li, L. Zou, B. Ye, Graphene blended with SnO2 and Pd-Pt nanocages for sensitive non-enzymatic electrochemical detection of H2O2 released from living cells, Anal. Chim. Acta. 1014 (2018) 10–18. doi:10.1016/J.ACA.2018.01.067.

[51] B. Ma, C. Kong, X. Hu, K. Liu, Q. Huang, J. Lv, W. Lu, X. Zhang, Z. Yang, S. Yang, A sensitive electrochemical nonenzymatic biosensor for the detection of H2O2 released from living cells based on ultrathin concave Ag nanosheets, Biosens. Bioelectron. 106 (2018) 29–36. doi:10.1016/J.BIOS.2018.01.041.

Figure Captions

Fig. 1: A) Cyclic Voltammetry of solutions containing, 5 mM Fe^{3+} and 5 mM $[Fe(CN)_6]^{3-}$ in a bare SPE (Blue and Green respectively) and SPE-CB (Black and Red respectively) recorded at 40 mV/s. B) Cyclic voltammograms electrodeposited PB on bare SPE (blue) and on SPE-CB (black) in 0.1M HCl and 0.1M KCl. Arrow indicate increasing number of growth cycles (5 and 20). Scan rate: 50 mV/s.

Fig. 2: SEM images of A) CB modified SPE B) CB/PB 5 cycles C) CB/PB 10 cycles D) CB/PB 20 cycles modified SPE.

Fig. 3: A) Peak current dependence with flow rate B) Hydrodynamic Voltamogramm (HDV) of a solution containing phosphate buffer (pH=7.4) (squares) and phosphate buffer (pH=7.4) and 10 µM of H_2O_2

Fig. 4: A) Signals in a FIA system to different concentrations of H_2O_2 B) Calibration plot for wide linear range. Inset: calibration plot for the lowest points. Measurements carried out in phosphate buffer (pH=7.4) flow rate 0.6 ml min^{-1}; E= -50 mV.

Fig.5: A) Amperometric signals due to the addition of FBS (1), L-Glu (2) and P/S (3) in DMEM medium B) Selectivity of the electrode towards 100 µM of H_2O_2 spiked in the cell culture without cells. E=-50 mV vs Ag

Fig. 6: Hydrogen peroxide concentration (black) and cell viability (blue) in Parkinson's disease cellular model at different incubation time

Figure 1

Click here to download high resolution image

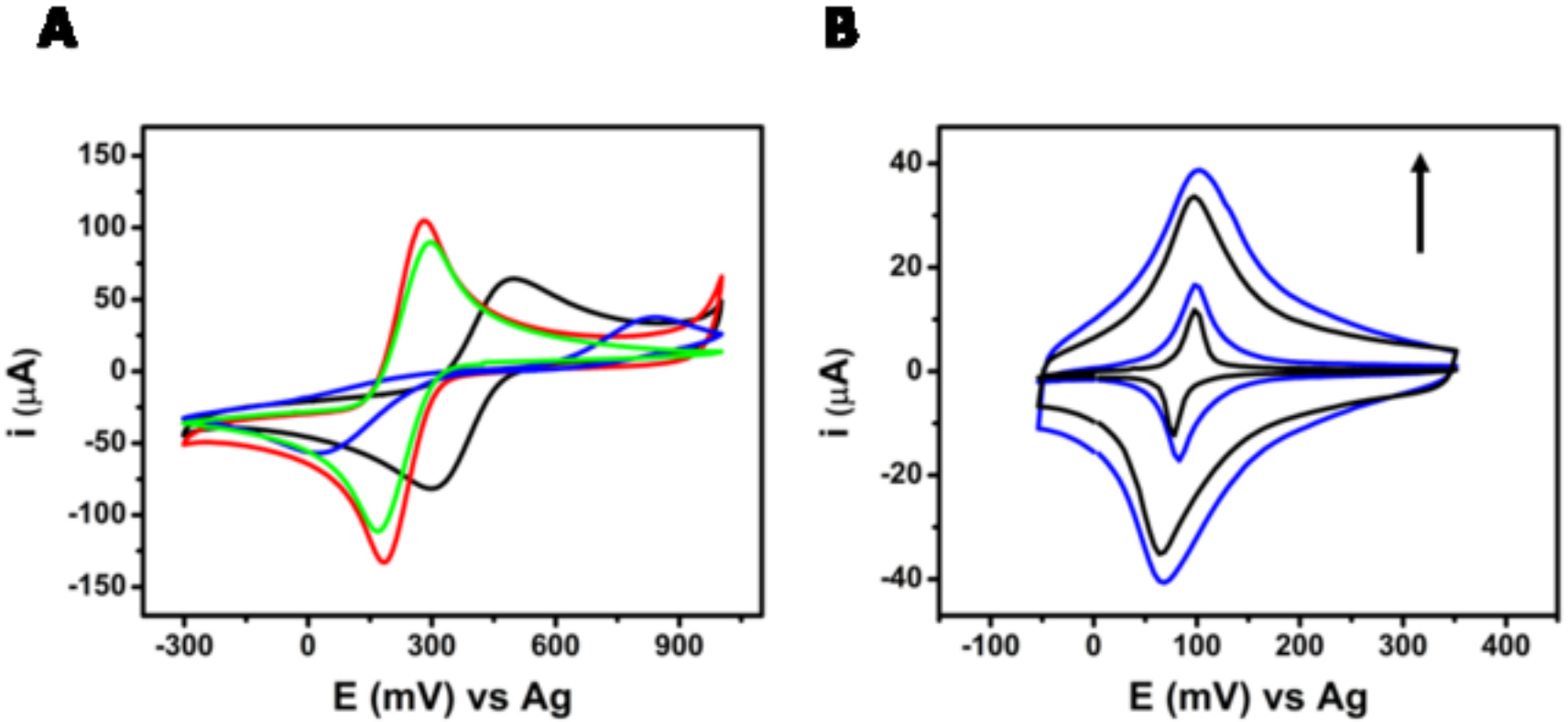

Figure 2

Click here to download high resolution image

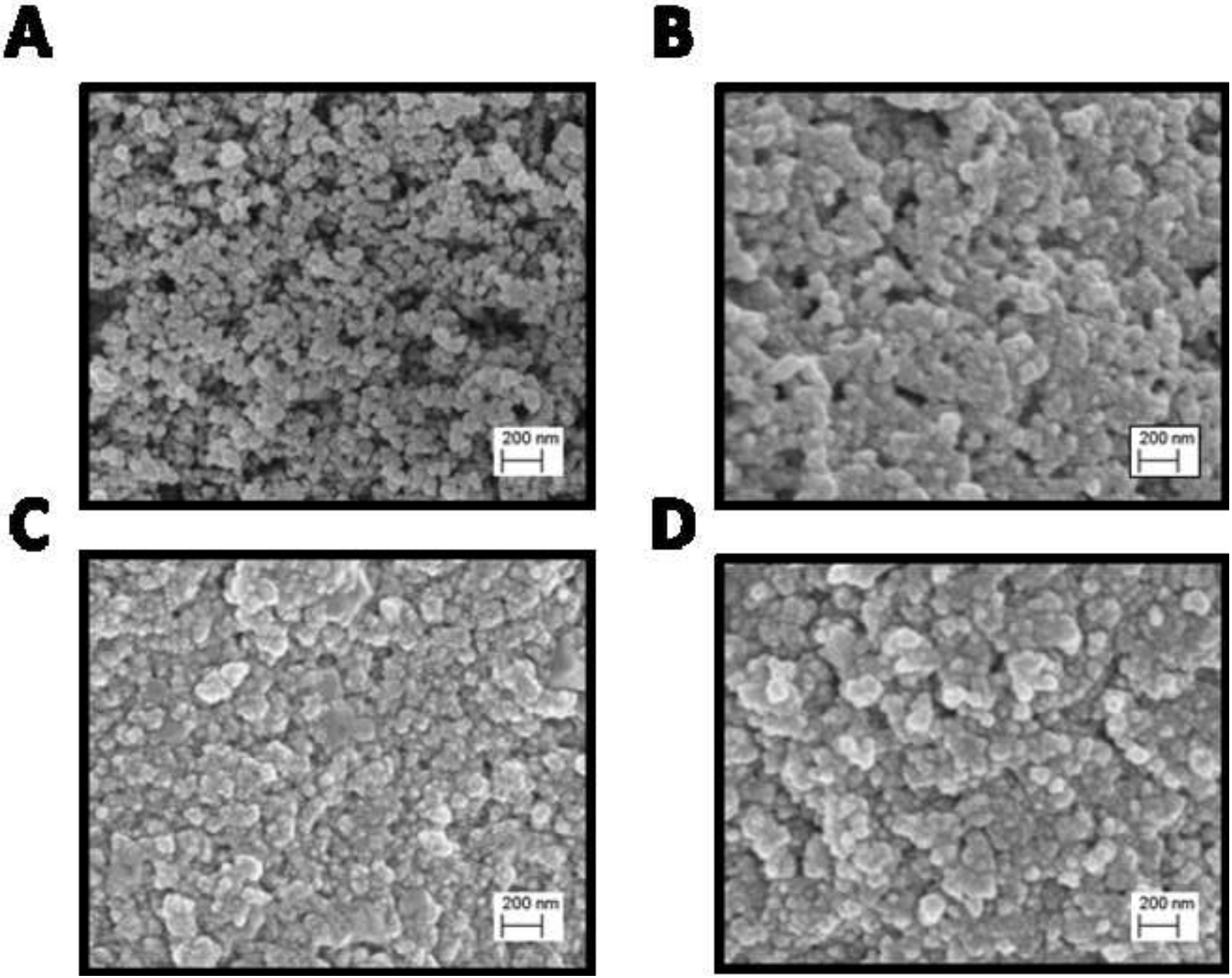

Figure 3

Click here to download high resolution image

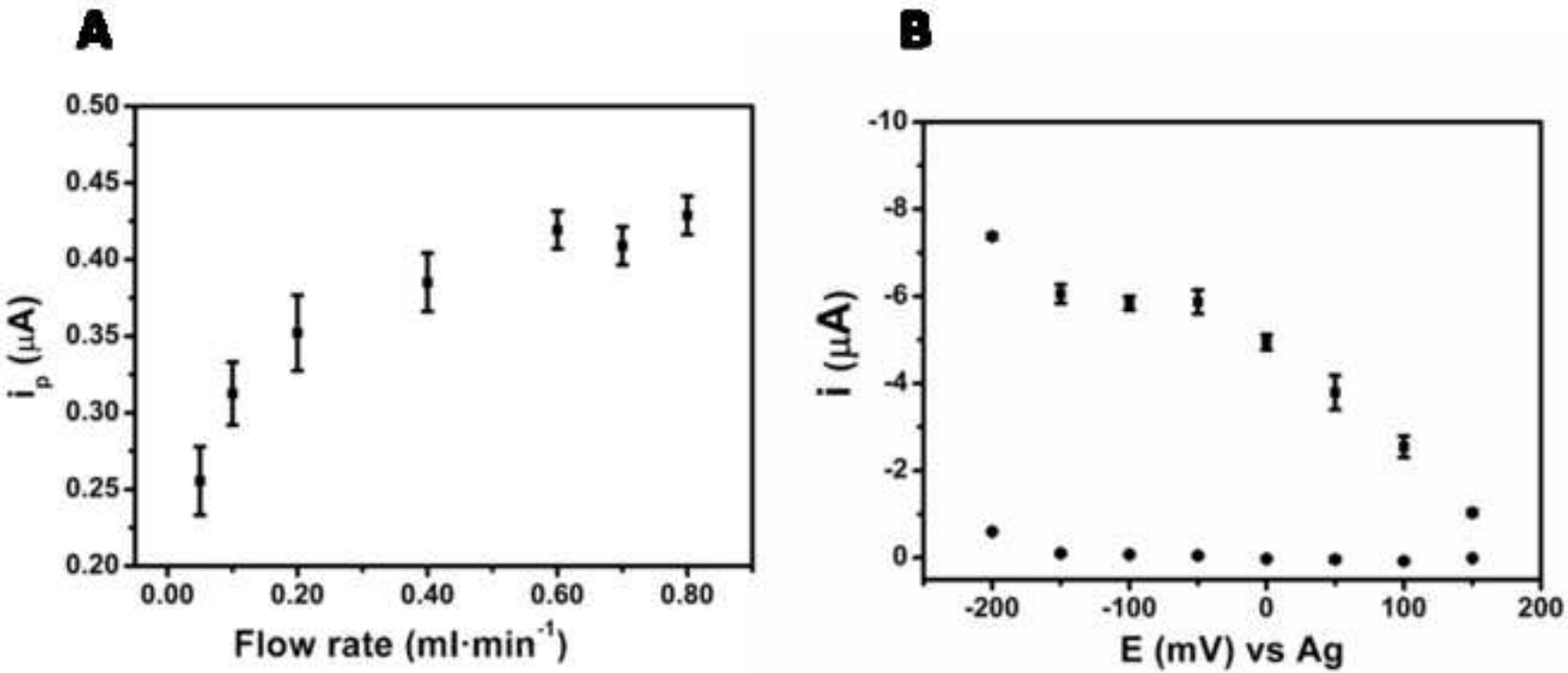

Figure(s)

Click here to download high resolution image

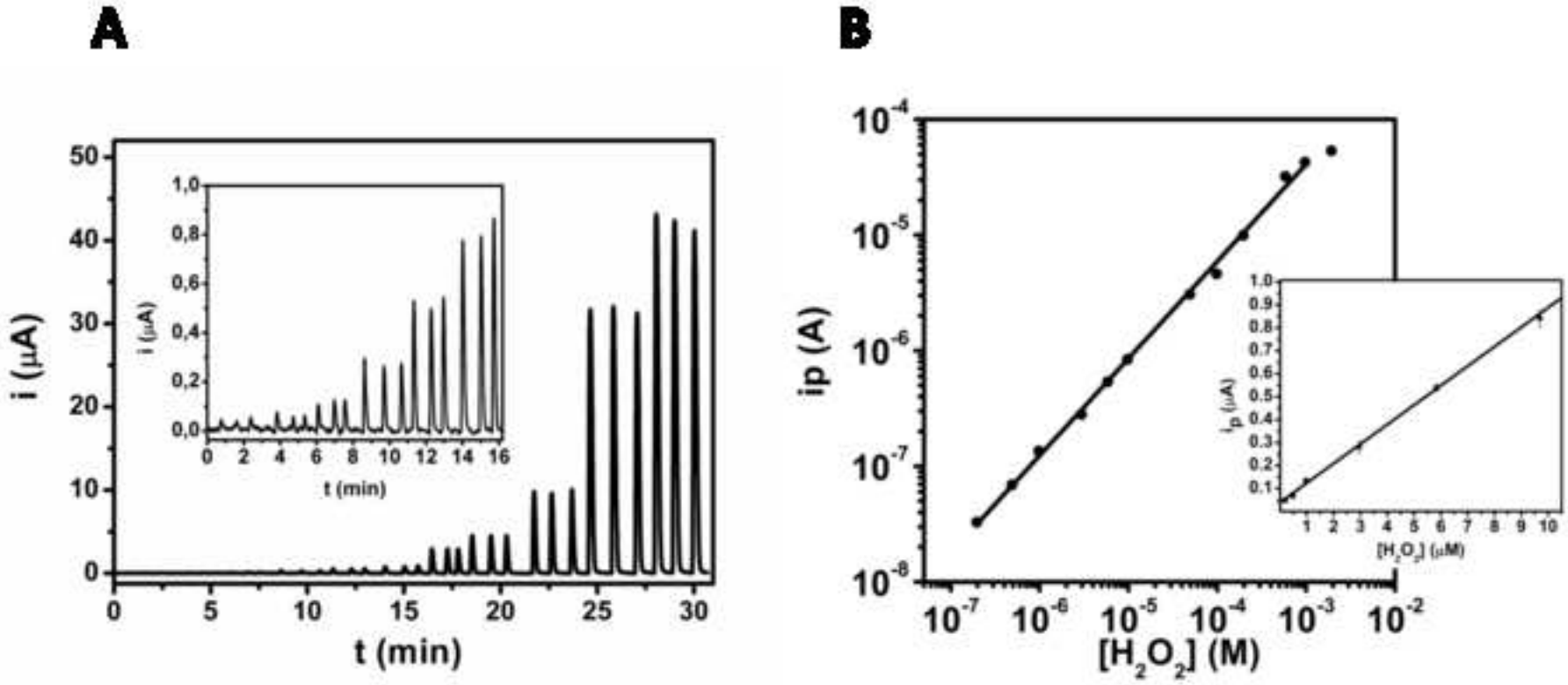

Figure 5

Click here to download high resolution image

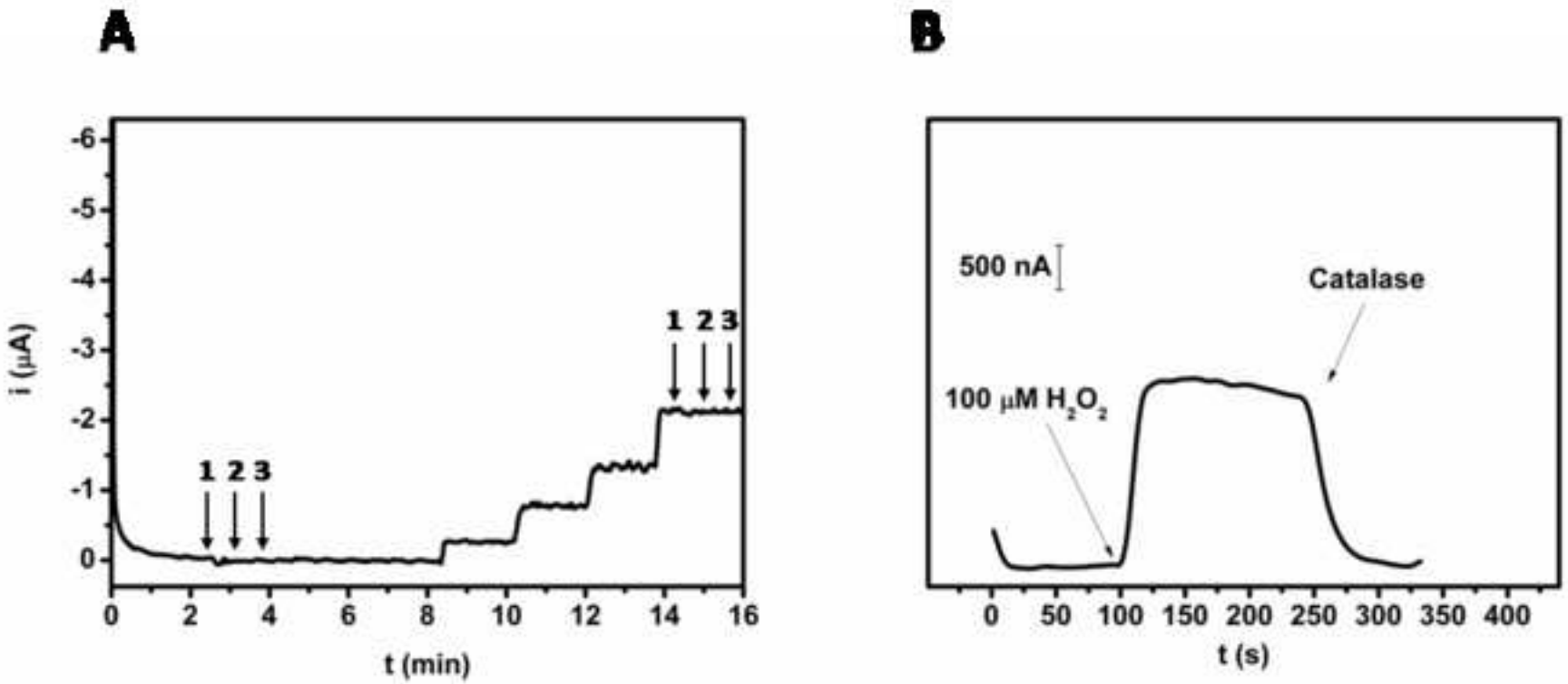

Figure 6

Click here to download high resolution image

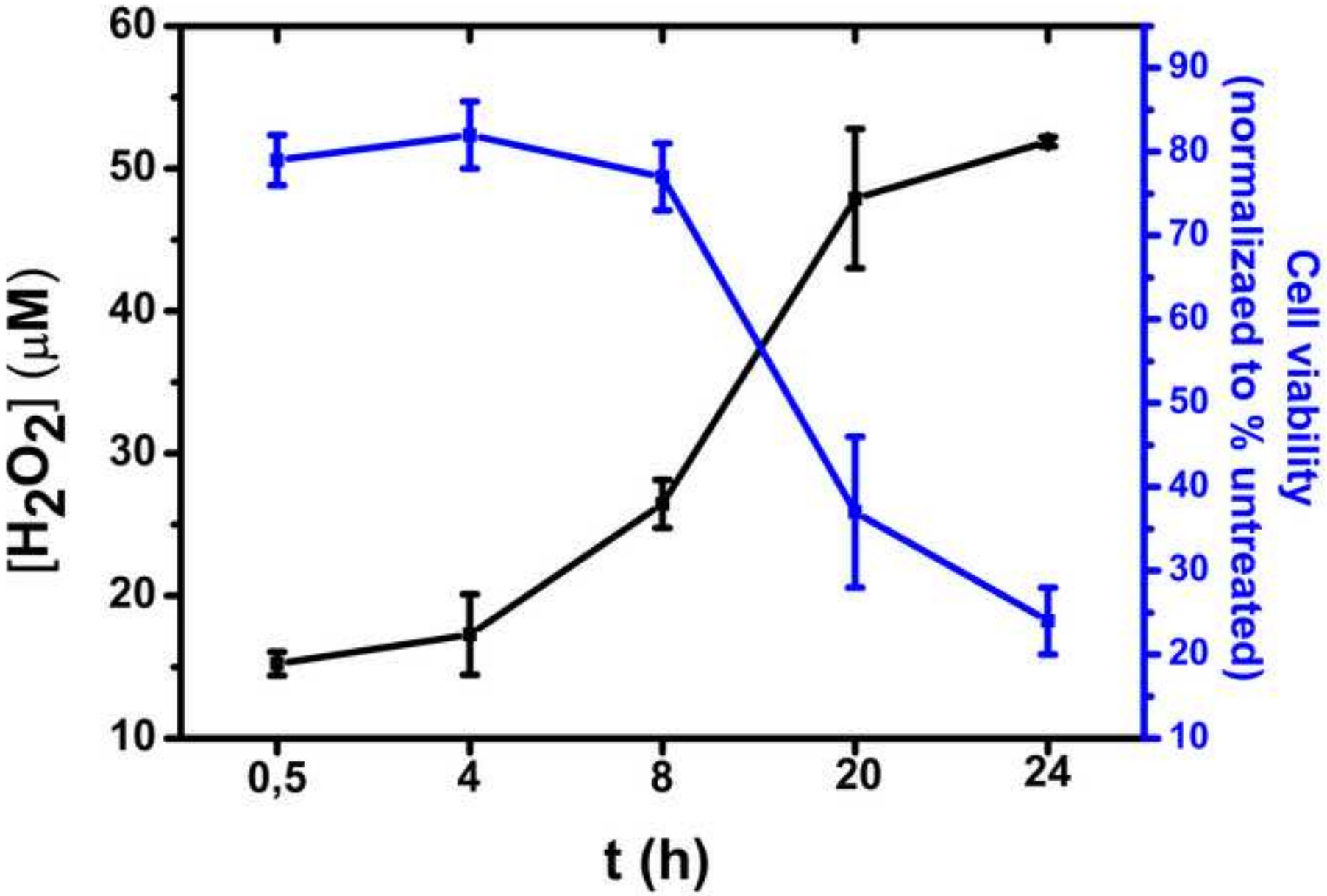

Supplementary Material

Click here to download Supplementary Material: Supplementary Information.docx

Daniel Rojas holds a bachelor's degree in Chemistry and master's degree in Electrochemistry. Nowadays, he is an Early Stage Researcher into Rep-Eat doctoral Programme and joint PhD student of Food Science at the University of Teramo and Chemistry at the University of Acalá. His current research interest is the characterisation and application of new nanomaterials for oxidative stress (bio)markers and polyphenols sensing.

Flavio Della Pelle is a postdoctoral researcher at the University of Teramo and achieved his PhD in Food science and analytical chemistry at the University of Teramo and at the University of Alcalá, respectively. He authored 22 publications in the analytical chemistry field. His research interest is focus on the development of robust and simple alternative analytical methodologies based on nanomaterials, for the 'assessment of the food quality and safety'.

Michele Del Carlo holds a PhD in Analytical Chemistry (University of Florence, Italy) and a Master of Science in Biosensors (University of Newcastle upon Tyne, UK). He is Associate Professor of Analytical Chemistry at the Faculty of Bioscience, University of Teramo; his main research interests are in the field of electrochemical sensors and biosensors for food safety and quality. In this area he has published more than 65 peer reviewed papers.

Michele d'angelo is a PhD student in molecular and cellular biotechnology. His main interest is neurodegenerative disease and the in vitro and in vivo models. Moreover, he worked with glioblastoma cancer cells, dissecting the molecular and cell pathway to better understand the pathology mechanism and to study a potential therapy treatment.

Reyes Dominguez-Benot holds a bachelor's degree in pharmacy and master's degree in Genetics. Nowadays she is an Early Stage Researcher into Rep-Eat Doctoral Programme and PhD student of Cellular and Molecular Biotechnology at the University of L'Aquila. The recent part of her research is devoted to understanding both the initiation and progression of tumours of the reproductive system and the role of Olive Leaf extract in Breast and Ovarian cancer and its effect on the cell cycle.

Annamaria Cimini is Full Professor of Cell Biology at the Department of Life, Health and Environmental Sciences, University of L'Aquila; her main research interests are in the field of Neurosciences with particular regard to neurodegenerative diseases and brain cancer. In this area she has published more than 85 peer reviewed papers. She is Co- inventor of 3 patents.

Alberto Escarpa is Professor of Analytical Chemistry at the University of Alcalá since 2003. His research activity is focused on microfluidics, biosensing, nanomaterials and micro motors. He has co-authored more than 110 peer-reviewed articles in international journals, yielding an h-index of 37, is the editor of two books. He has given more than 20 invited talks in highly international meetings about microfluidics and miniaturization of analytical chemistry. He is also Associate Editor of Microchimica Acta, RSC Advances and Electrophoresis and member of the Editorial board of Electrophoresis, Food Chemistry, Applied

Materials Today and Microchimica Acta. He is also member of Royal Society of Chemistry since 2016.

Dario Compagnone has coordinated in the last 10 years the analytical chemistry group of the Faculty of Biosciences of the University of Teramo. He is author of over 160 papers on international scientific journals. His research interests are focussed on the development of sensing and biosensing strategies for the rapid detection of quality and safety markers of food.

***Research Highlights**

- An enzyme-free Carbon Black-Prussian Blue based electrochemical sensor for H_2O_2 sensing is proposed
- Carbon Black successfully assist the electrodeposition of Prussian Blue
- Interference-free H_2O_2 direct quantification in cell cultures has been achieved
- The proposed sensor has been applied to H_2O_2 monitoring in 6-OHDA cellular model of Parkinson's disease